Article

TRANSCRIPTION FACTOR Bmsage PLAYS A CRUCIAL ROLE IN SILK GLAND GENERATION IN SILKWORM, *Bombyx mori*

Hu-hu Xin, Deng-pan Zhang, Rui-ting Chen, Zi-zheng Cai, Yan Lu, Shuang Liang, and Yun-gen Miao

Institute of Sericulture and Apiculture, College of Animal Sciences, Zhejiang University, Hangzhou, People's Republic of China

Salivary gland secretion is altered in Drosophila embryos with loss of function of the sage gene. Saliva has a reduced volume and an increased electron density according to transmission electron microscopy, resulting in regions of tube dilation and constriction with intermittent tube closure. However, the precise functions of Bmsage in silkworm (Bombyx mori) are unknown, although its sequence had been deposited in SilkDB. From this, Bmsage is inferred to be a transcription factor that regulates the synthesis of silk fibroin and interacts with another silk gland-specific transcription factor, namely, silk gland factor-1. In this study, we introduced a germline mutation of Bmsage using the Cas9/sgRNA system, a genome-editing technology, resulting in deletion of Bmsage from the genome of B. mori. Of the 15 tested samples, seven displayed alterations at the target site. The mutagenesis efficiency was about 46.7% and there were no obvious off-target effects. In the screened homozygous mutants, silk glands developed poorly and the middle and posterior silk glands (MSG and PSG) were absent, which was significantly different from the wild type. The offspring of G_0 mosaic silkworms had indel mutations causing 2- or 9-bp deletions at the target site, but exhibited the same abnormal silk gland structure. Mutant larvae containing different open-reading frames of Bmsage had the same silk gland phenotype. This illustrated that the mutant phenotype

Grant sponsor: National Basic Research Program of China; Grant number: 2012CB114601; Grant sponsor: National Natural Science Foundation of China; Grant number: 31372374/C1703; Grant sponsor: Chinese Universities Scientific Fund.

Correspondence to: Yun-gen Miao, College of Animal Sciences, Zhejiang University, Hangzhou 310058, P. R. China. E-mail: miaoyg@zju.edu.cn

ARCHIVES OF INSECT BIOCHEMISTRY AND PHYSIOLOGY, Vol. 0, No. 0, 1–11 (2015)
Published online in Wiley Online Library (wileyonlinelibrary.com).
 DOI: 10.1002/arch.21244

was due to Bmsage knockout. We conclude that Bmsage participates in embryonic development of the silk gland. © *2015 Wiley Periodicals, Inc.*

Keywords: silkworm; *Bmsage*; transcription factor; silk gland; development

INTRODUCTION

The silk gland is vitally important for silkworm, *Bombyx mori* as its uniqueness biosynthesizing the silk protein and spinning the silk fiber. The silkworm synthesizes fibroin and sericin proteins in silk gland to cocoon and pupate inside that shelter at the mature stage. In silk industry, the silk output and quality directly depend on the growth and development of silk gland. As a promising bioreactor, the silk gland also has been used to generate exogenous proteins such as vaccine (Xu et al., 2014), enzyme (Wang et al., 2013a), etc., at advantage of its high yield and low expense. Consequently, studies on gene function and synthesis mechanism of silk protein have become a hotspot in modern biology.

The silk gland that derives from the specialized labium gland locates on left and right side of digestive tube and composes of anterior silk gland (ASG), middle silk gland (MSG), and posterior silk gland (PSG). The silk gland grows in a rapid speed from hatch to maturity, resulting in the size increase by thousands of times. This rapid growth is the result of enlargement of the silk gland cells thoroughly, as the cells stop dividing after silk gland generated in the embryonic period (Goldsmith et al., 1984). It has been known that silk gland originates from the invaginated ectoderm and has its whole structure before hatch (Kokubo et al., 1996). Although the complete genome sequence of silkworm has been available (Xia et al., 2009), the molecular mechanism of silk gland development during embryonic stage has not been understood clearly. *B. mori sage (Bmsage*) homologous to *Drosophila sage* is a special gene, which expressed mainly in the MSG and PSG during larva stage. The Bmsage protein is a transcription factor carrying a basic helix-loop-helix (bHLH) domain and binding to the A and B elements in the promoter of *fibroin H-chain* gene (*fib-H*) to regulate the synthesis of silk fibroin, interacted with another gland-specific transcription factor silk gland factor-1 (SGF-1) during that process (Zhao et al., 2014). Moreover, silk gland of *Bombyx mori* is regarded as homologous organ to salivary gland of *Drosophila*, and *sage* plays a major role in the generation and development of salivary gland (Rebecca et al., 2013). It is required in the formation of secretary tube and maintenance of a uniform and patent lumen through regulating the two downstream target genes *PH4*α*SG1*and *PH4*α*SG2* together with Fork head (Fkh) (Abrams et al., 2006). Therefore, we speculate that *Bmsage* is also one decisive gene in silk gland formation.

In this study, we used the flourishing genome editing technology CRISPR (clustered regularly interspaced short palindromic repeats) with an associated protein (Cas9) system that has been successfully applied in many model organisms including *Bombyx mori* (Wang et al., 2013b; Daimon et al., 2014; Ma et al., 2014; Liu et al., 2014; Wei et al., 2014).We designed the specific target for *Bmsage*, synthesized high quality Cas9-mRNA and sgRNA in vitro and injected into the new hatched eggs to destroy its function of *Bmsage*. In the screened homozygous mutants, the silk glands that developed poorly and MSG and PSG parts were absent, which was significantly different from wild type. This phenomenon was further confirmed by dissecting and sequencing. We concluded that the *Bmsage* participated in the development of silk gland at embryonic stage.

MATERIALS AND METHODS

Silkworm Strain

The silkworm P50 strain was maintained at Zhejiang University (Hangzhou, China), and reared on fresh mulberry leaves under conventional condition of 25 °C, 75% RH. It was treated for preventing diapause according to (Zhao et al., 2012) method.

Sequence Confirmation and Target Design for **Bmsage** *Gene*

According to the sequence of *Bmsage* (Gene ID: BGIBMGA005127-TA) in the SilkDB (http://silkworm.genomics.org.cn/), a pair of primer was used for PCR amplification as following: forward primer: 5′-ATGTACAATCAAACATAC-3′; reverse primer: 5′-TTAGATTCTCTGTTGACG-3′. The PCR product was cloned into T vector, and sequenced. The introns and exons of *Bmsage* were analyzed using the Sim4 program (http://doua.prabi.fr/software/sim4), and the key domain was predicted through SMART program (http://smart.embl-heidelberg.de/).

Upon the confirmed *Bmsage* sequence, we designed one target in or near the key domain sequence for Cas9 according to our previous description (Yu et al., 2013; Wei et al., 2014), that is 5′-GGG/A-N17/18-NGG-3′ located in the exon (Table S1). A 320-bp fragment around the target was amplified using another pair of primer (forward primer: 5′-TCAGGTCCGCGTTACTATGAGCA-3′; reverse primer: 5′-CGCTGCGAGAATGTCACAAATAT-3′) to confirm that the above target sequence is identical in the genome of silkworm.

Microinjection of Silkworm Embryos

In this study, pSP6-2sNLS-SpCas9 and pMD19-T sgRNA scaffold plasmids were received from Tsinghua University. The Cas9-mRNA was synthesized *in vitro* against the vector pSP6-2SNLS-spcas9 using a SP6 mMESSAGE mMACHINE Kit (Ambion, USA) (Wei et al., 2014). And the Poly(A) signal was added to the 3′ of capped mRNAs above by *Escherichia coli* Poly(A) polymerase Kit (New England BioLabs, USA).The customized sgRNAs were prepared as previously described (Chang et al., 2013; Cho et al., 2013) with transcription performed using a RiboMAX Large Scale RNA Production Systems-T7 Kit (Promega, Madison, WI, USA).

The newly hatched eggs were collected within 1 h after ovipositing, disinfected for 3 min in 1% formaldehyde, and then, rinsed three times by sterile water. The treated eggs were scheduled for microinjection within 4 h. The injection was performed in Nikon NARISHIGE NT-88-V3 microinjector coupled with Nikon SMZ645 microscope. The Cas9-coding mRNA and sgRNA were mixed at final concentrations of 500 ng/μl and 250 ng/μl (about 2–3nl/egg), respectively. The injected eggs were incubated at 25°C, 75% RH for 9–10 days until hatching.

Mutation Screen and Phenotype Analysis

Firstly, we calculated the efficiency of Cas9/sgRNA-mediated gene alteration in the injected generation (G_0). We collected individual specimens 5 days after injection to extract genomic DNA for PCR using the above primers and sequenced the PCR product directly (316 bp). The multiple peaks in chromatograms of PCR-product sequencing at a base

position were indicative of mutation. Then the PCR product containing mixed-individual mutations was TA-cloned and sequenced to determine the exact mutation type.

Then, we conducted the Cas9/sgRNA-mediated mutation screens. Due to the uncertainty of the phenotype of loss-of-function mutations in *Bmsage*, we looked for the veritable phenotype from several possibilities. According to the function of *sage* in *Drosophila*, we speculated that *Bmsage* is correlated with the generation or/and development of silk gland. In this case, silk glands from the *Bmsage*-mutated individuals were dissected and observed. The silkworms with abnormal silk glands were screened for further validation.

Crossing Strategies

Bmsage is located on the euchromosome (Chr.25) (Zhao et al., 2014). To obtain the homologous mutants (two allele mutations) quickly, the same crossing strategies stated in our previous study were utilized (Wei et al., 2014). The mosaic of the injected generation (G_0) was crossed with each other. In addition, the frequency of germline transmission in G_1 was evaluated by G_0 mosaic crossed with uninjected wild type.

Potential Off-Targeting Detection

The potential off-targeting effect of *Bmsage* target loci against the whole silkworm genome was evaluated using CasOT searching tool (Xiao et al., 2014), and then, PCR amplification to the corresponding off-target sites and DNA sequencing were performed for the further evaluation of off-targeting effect.

RESULTS

Verification of Bmsage Target Sequence

The genomic sequence of *Bmsage* was synthesized by PCR and sequenced. Based on the information of *Bmsage* from SilkDB, we verified its sequence and homozygosity. The genomic full-length of *Bmsage* is 2435 bp, composed of four exons and three introns, and Bmsage protein contains one key domain, bHLH, in third and fourth exons, predictably. We designed a target for CRISPR/Cas9 in the second exon (Fig. 1A), sequencing result showed the candidate target sequence is a homozygosity in P50 strain we used.

Bmsage Was Destroyed With High Efficiency and Specificity

The embryos of G_0 generation injected with a mixture of Cas9-mRNA and *Bmsage*-tar sgRNA were detected to assess mutagenesis efficiency by single embryo. The multiple peaks in chromatograms of PCR-product sequencing at a base position indicated the mutation (Fig. 1B). In this study, 7 from 15 tested samples displayed alterations at the target site. Its mutagenesis efficiency was about 46.7% (7/15) (Table 1).

The frequency of germline mutation transmission (mutation transmitting from G_0 to G_1) was evaluated through G_1 offspring. *Bmsage* mosaic G_0 moths were crossed with wild-type moths. In this cross, 9 of 12 G_1 larvae contained one mutant sister chromatid and one wild type (75%, 9/12). However, the transmission frequency of another crossing strategy (G_0 mosaic × G_0 mosaic) was a little lower (29.4%, 15/51) (Table S2).

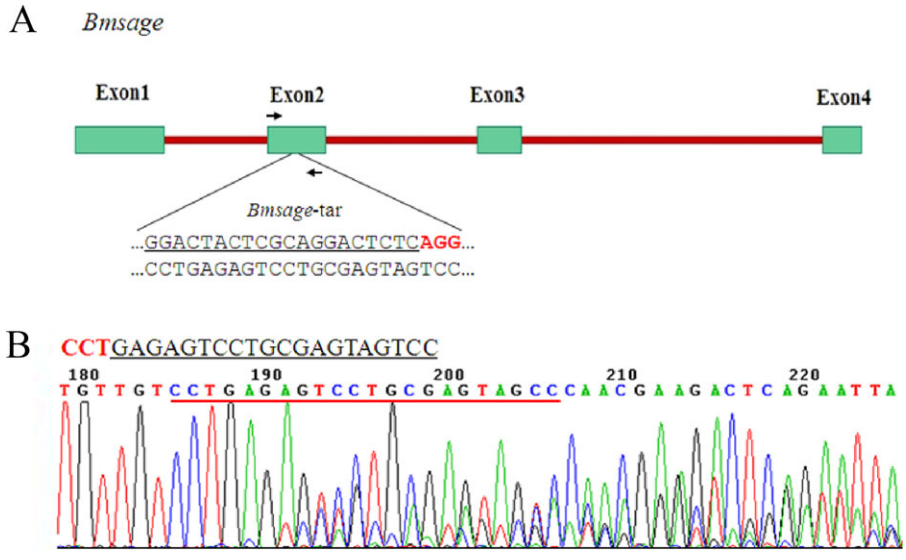

Figure 1. Schematic representation of *Bmsage* and representative chromatograms of PCR-product sequencing in injected G_0 silkworms. (A) Exons are shown as boxes and arrows represent the primers used to amplify the target region. (B) The multiple peaks near the target declared the mutation happened. Target site (*Bmsage*-tar) is underlined. PAM sequence is bold in red.

Table 1. Mutations Induced by Cas9/sgRNA Microinjection in G_0

Target gene	*Embryos Injected (n)*	*Total sequencing number (n)*	*Mutant number by sequencing (n)*	*Frequency of mutation in G_0*
Bmsage	296	15	7	46.7% (7/15)

To estimate the off-targeting effect, we searched all the potential off-target sites of *Bmsage* target locus using the CasOT searching tool in the whole silkworm genome. Seven most similar sites selected from the search results were further proceed to test by PCR amplification using the genome template of injected G_0 silkworms. The sequencing results revealed no obvious off-targeting effects (Fig. S1).That implied the high specificity of the selected *Bmsage* target using our Cas9/sgRNA system.

Bmsage Mutant Phenotype

There is no public report about mutant phenotype of *Bmsage* gene caused by genome editing technique, and no natural mutant. It is an evident challenge to seek the potential phenotype of loss-of-function silkworm in *Bmsage*. During our screening process, no abnormal appearance differed with wild type was observed in the G_0 and G_1 larvae, even though silk glands were dissected from some larvae. Until to G_2, we found that a few mature silkworms were unable to spin silk and build cocoons, finally most of them died on account of losing pupating ability.

We dissected all the dead non-silk-larvae and found that their silk glands deformed absolutely. Further observation showed that the abnormal silk glands were short of MSG and PSG, only the whole ASG and a small part of PSG remained (Fig. 2C–E). The wild-type

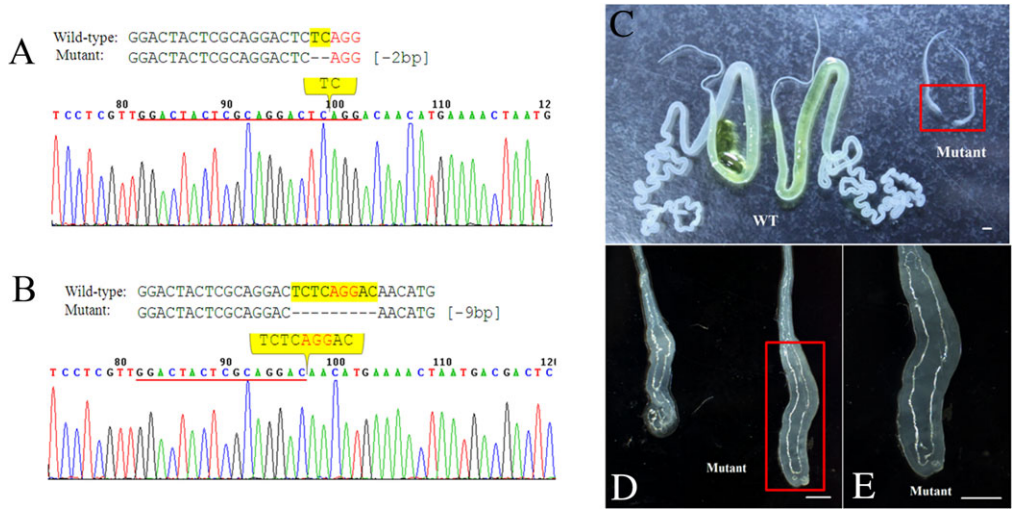

Figure 2. Two kinds of indel mutations separated from offspring of G_0 mosaic silkworms and their silk glands phenotype. (A) and (B) *Bmsage* mutant sequences with 2-bp and 9-bp deletion at target site, respectively. The deleted nucleotides are highlighted in yellow. PAM is highlighted in red. The target is underlined by red in chromatograms (-, deletion). (C), (D), and (E) Silk glands from WT and *Bmsage* mutant silkworms on day 6 of fifth instar. (C) shows the whole structures of WT and mutant silk glands photographed by Canon EOS 500D. (D) is another magnified picture from the red box in (C) and (E) magnified from (D). The two pictures were photographed by Nikon Az100 microscope. WT silk gland had the integrated structure including ASG, MSG and PSG in (C). However, mutant silk gland only retained ASG and a small part of MSG. The residual MSG of mutant silk gland was distorted in (E). The scale bars represent 1 mm.

silk gland consists of a linear ASG and a *Z*-shaped MSG followed by a longest curved PSG (Fig. 2C). It can be seen that the lack of MSG and PSG gave rise to the inability of spinning directly, as the mutants were unable to synthesize fibroin and sericin proteins.

To verify whether this phenotype is related to the function loss of *Bmsage*, all the non-silk-larvae were sequenced in G_2. Consequently, they had the same genotype of 2-bp deletion at target site (Fig. 2A), and all were homozygote. However, other individuals with normal silk gland displayed wild-type or heterozygous genotype (one wild-type and one mutant). As a result, we preliminarily concluded that loss-of-function mutant was caused by *Bmsage* knockout.

The Silk Gland Generated Abnormally in Bmsage *Mutant Larva*

The silk gland forms completely during the period of embryonic development. We speculated that the silk gland abnormality began at the late embryonic stage due to *Bmsage* knockout. There is just size increasing of silk gland from newly hatched larva to mature stage. To confirm it, we checked larva since it was old enough to be dissected. As a result, first molting larva (first instar larva) had no MSG and PSG except for ASG and a small part of MSG (Fig. 3A). In this mutant, the end of silk gland was a blind tube (Fig. 3B). Additionally, the residuary cells of MSG presented distorted shape, irregular arrangement, and no distinct tube for secreting and storing silk proteins formed (Fig. 3D). For the above structural defect of silk gland, mutant larva cannot spin any silk after maturity, and eventually, became naked pupa entirely.

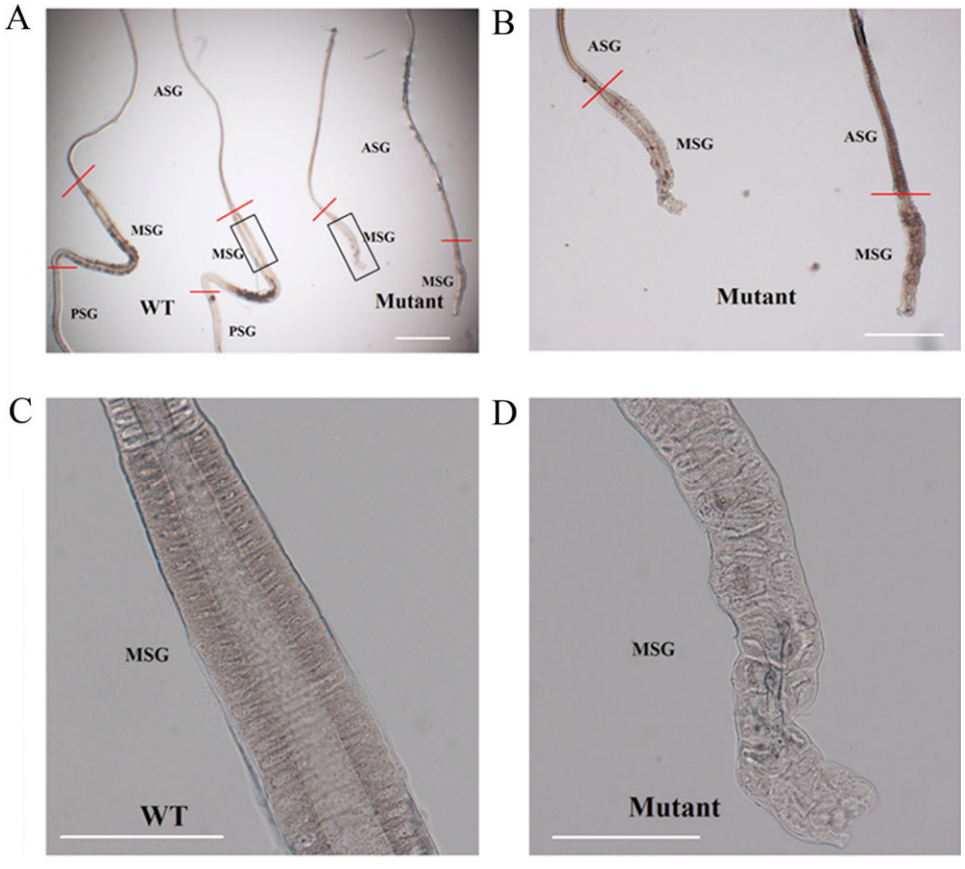

Figure 3. Silk glands of first instar larvae from WT and *Bmsage* mutant. (A) The whole view of WT and mutant silk glands of first instar larvae. (B) is magnified mutant silk gland from (A). (C) and (D) are amplified from the box region in (A) respectively. ASG, MSG, and PSG are separated by red lines. Like the silk gland of fifth instar larva in Fig. 2, the first instar larva also had resembled structure of silk gland. In addition, the MSG cells were irregular arrangement in mutant silk gland in (D). The scale bars represent 1 mm. All pictures were photographed by Nikon Az100 microscope.

Different Indel Mutations Displayed the Same Phenotype

For further investigating this causal relationship between deficiency of *Bmsage* function and structural deformity of silk gland, we separated two different kinds of indel mutations from offspring of G_0 mosaic silkworms. One was 2-bp-deletion at target site as showed in Fig. 2A. Another indel mutation was 9-bp-deletion at target site as showed in Fig. 2B. The silk glands from both indel mutations had same abnormal structure. In other words, the mutant larvae containing different ORFs of *Bmsage*, which caused frame shift of *Bmsage* sequence, displayed the same mutant silk gland phenotype. This illustrated that the mutant phenotype was the result of *Bmsage* knockout.

Mutant Larvae Growth During Pupating

In G_2 mutant silkworms, most larvae died at the pupation stage. Some of them were unable to pupate completely, and their whole body softened, keeping the larvae form (Fig. 4A).

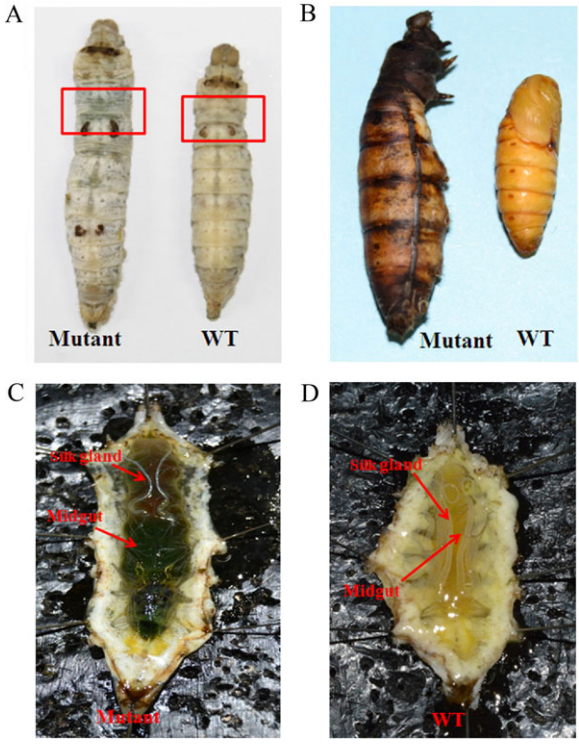

Figure 4. The mutant silkworm phenotype from larva to pupating. (A) The mutant and WT of matured larva. The mutant cannot pupate and died with the whole body soften and full of mulberry leaves in the gut (Light green color of mulberry leaves can be seen in the red box of the mutant). (B) The mutant and WT pupae. The mutant pupa was bigger than WT pupa and displayed deformity characteristic. (C) and (D) The anatomical appearances of mutant and WT mature larvae. All pictures were photographed by Canon EOS 500D.

Some can begin pupating, but stop at the initial stage. In these uncompleted pupae, their heads, thoraxes and thoracic legs still retained as larva phenotype. But the abdomen had taken on pupal morphology with its size greater than normal dramatically. These abnormal pupae maintained this shape until died accompanying with darkening (Fig. 4B).

The Survival Mutant Pupa can Emerge Into Moth, Mate and Oviposit

Though most mutants died during pupation, some also can survive to emerge. Interestingly, the survival mutants can become pupae without spinning silk. When the mutants matured, they had the same behavior of spinning (shaking head) but no cocoon making. Like wild-type silkworms, 3 days after maturity the mutants became pupae without cocoon packed. And about 6 days later the naked mutant pupae emerged into moths. Same as wild-type moths, the mutant moths can mate with each other and lay eggs naturally. Now we had raised the *Bmsage*-mutant silkworm to G_7 generation, so *Bmsage* knockout cannot affect silkworm fecundity.

DISCUSSION

For the first time, we obtained the knockout silkworm of *Bmsage* gene using CRISPR/Cas9 gene editing system, and found its phenotype of deformed silk gland with MSG and PSG absent. This mutant silkworm cannot spin and make cocoon when they become mature, with high mortality rate during pupation, only a few of them can metamorphose and oviposit successfully.

At present only a few papers using the CRISPR/Cas9 technique with *B. mori* were screened, mainly as a model system to show the application of the technique in silkworm (Wang et al., 2013b; Daimon et al., 2014; Ma et al., 2014; Liu et al., 2014; Wei et al., 2014). This is the first time to exploit the method to generate a mutation in a gene with unknown function.

Like ZFN and TALEN, CRISPR/Cas9 system is defective as well although it has become one powerful genome engineering technology. Off-targeting is a potential issue about the application of Cas9/sgRNA technology in genome editing. It has been reported that PAM type and mismatch site from the seed region or nonseed region have an influence on the specificity of the CRISPR/Cas9 system (Cradick et al., 2013; Fu et al., 2013; Hsu et al., 2013; Pattanayak et al., 2013). Thus, the potential off-targeting effect of *Bmsage* target loci against the whole silkworm genome was evaluated using CasOT searching tool. The sequencing results revealed no obvious off-targeting effects, which implied the high specificity of the selected *Bmsage* target. Two kinds of indel mutations from offspring of G_0 mosaic silkworms displayed 2-bp deletion and 9-bp deletion at target site respectively, but presented the same abnormal structure of the silk glands. The mutated larvae containing different ORFs of *Bmsage* displayed the same phenotype of silk gland. This illustrated that the mutant phenotype was the result of *Bmsage* knockout.

Naturally, the redundant leaves are excreted in form of faeces and urine before pupating, the silk proteins are spit out from silk gland to make cocoon. In one word, wild-type larva can pupate safely only after all wastes are excluded (Fig. 4D). On the other hand, similar to the malpighian tubule, silk gland could be regarded as an excretory organ used for expelling spare amino acids in form of spinning, avoiding lethality that comes from excessive amino acids accumulation. Whereas *Bmsage* mutant has no synthesized silk because of uncompleted silk gland, no too much amino acid accumulation in body. So we guessed that the death is not aroused by amino acid poisoning. This speculation also can be proved by the survived mutant moths.

Dissecting those died mutants made us know that their guts were full of indigested leaves that have already begun fermenting with unpleasant odor (Fig. 4C). The lethality was extremely high, 12 in all the 19 mutants of G_2 were dead, and the others pupated normally. In G_3 mutants, only one pupated at last from one brood of 11 mutants. For the direct death reason, we supposed that it maybe associate with the vast indigested mulberry leaves in the guts. The leaves larva took during the larva stage will not be digested to produce silk proteins or be removed from body actively, and eventually, fermented slowly, resulting in the larva death. But at present we cannot get the detailed reason of death profoundly. From the above discussion, we can discover that the big difference between survival mutants and lethal mutants was whether mulberry leaves remained in guts of mature larvae.

Obviously, the mutant larva does not need more mulberry leaves than wild-type larva. Accordingly, we thought that less leaves will meet the demand of mutant larva maturing, especially during fifth instar. Whether feeding less leaves can improve survival rate or not needs to be further tested. However, we tried giving less leaves (compared to the normal

amount) to one brood of mutant larvae of fifth instar and even no leaves feeding at the last two days, as a result, 54 mature larvae from total 72 pupated successfully (compared to 7 pupated larvae in 19 mutants in another brood).

The wild-type silkworm body reaches to the largest size at mature stage of fifth instar that mainly determined by the size of silk gland (especially MSG and PSG). At this stage silk gland size is also largest and takes up 40–50% weight of the whole larva (Grzelak et al., 1995). The *Bmsage* mutant larva loses the major parts of silk gland (MSG and PSG), so it should be smaller without the volume of silk gland. Interestingly there was no apparent difference between mutant and wild type in size when mixed them in one brood. Then, we could distinguish the mutant silkworm from wild type not by appearance but by silk gland dissection or observation of its spinning behavior. Furthermore, no obvious difference in size is due to the remaining mulberry leaves in the gut of mutant larva. We can also suppose that these remaining leaves would have been used to produce silk proteins, but the mutant was unable to utilize them.

In conclusion, *Bmsage* was involved in the embryonic development of silk gland, and played an essential role in the generation of silk gland. The *Bmsage* mutant silkworm kept deformed silk gland and lost MSG and PSG. This led to failure of spinning and cocoon formation. At the same time, because of the changes in absorption and metabolism of nutrients, especially amino acids, most mutants died except for a couple of normal pupae. Also, it is a fact that silk gland is not a necessary organ in silkworm life cycle.

REFERENCES

Abrams EW, Mihoulides WK, Andrew DJ. 2006. Fork head and Sage maintain a uniform and patent salivary gland lumen through regulation of two downstream target genes, *PH4αSG1* and *PH4αSG2*. Development 133:3517–3527.

Chang N, Sun C, Gao L, Zhu D, Xu X, Zhu X, Xiong J, Xi J. 2013. Genome editing with RNA-guided Cas9 nuclease in Zebrafish embryos. Cell Res 23:465–472.

Cho SW, Kim S, Kim JM, Kim JS. 2013. Targeted genome engineering in human cells with the Cas9 RNA-guided endonuclease. Nat Biotechnol 31:230–232.

Cradick TJ, Fine EJ, Antico CJ, Bao G. 2013. CRISPR/Cas9 systems targeting b-globin and CCR5 genes have substantial off-target activity. Nucleic Acids Res 41:9584–9592.

Daimon T, Kiuchi T, Takasu Y. 2014. Recent progress in genome engineering techniques in the silkworm, *Bombyx mori*. Dev Growth & Differ 56:14–25.

Fu Y, Foden JA, Khayter C, Maeder ML, Reyon D, Joung JK, Sander JD. 2013. High-frequency off-target mutagenesis induced by CRISPR-Cas nucleases in human cells. Nat Biotechnol 31: 822–826.

Goldsmith MR, Kafatos FC. 1984. Developmentally regulated genes in silkmoth. A Rev Genet 18:443–487.

Grzelak K. 1995. Control of expression of silk protein genes. Comp Biochem Physiol B Biochem Mol Biol 110:671–681.

Hsu PD, Scott DA, Weinstein JA, Ran FA, Konermann S, Agarwala V, Li Y, Fine EJ, Wu X, Shalem O, Cradick TJ, Marraffini LA, Bao G, Zhang F. 2013. DNA targeting specificity of RNA-guided Cas9 nucleases. Nat Biotechnol 31:827–832.

Kokubo H, Xu PX, Xu X, Matsunami K, Suzuki Y. 1996. Spatial and temporal expression pattern of *Bombyx fork head/SGF-1* gene in embryogenesis. Dev Genes Evol 206:80–85.

Liu Y, Ma S, Wang X, Chang J, Gao J, Shi R, Zhang J, Lu W, Liu Y, Zhao P, Xia QY. 2014. Highly efficient multiplex targeted mutagenesis and genomic structure variation in *Bombyx mori* cells using CRISPR/Cas9. Insect Biochem Mol Biol 49:35–42.

Ma S, Chang J, Wang X, Liu Y, Zhang J, Lu W, Gao J, Shi R, Zhao P, Xia QY. 2014. CRISPR/Cas9 mediated multiplex genome editing and heritable mutagenesis of *BmKu70* in *Bombyx mori*. Sci Rep 4:4489.

Pattanayak V, Lin S, Guilinger JP, Ma E, Doudna JA, Liu DR. 2013. High-throughput profiling of off-target DNA cleavage reveals RNA-programmed Cas9 nuclease specificity. Nat Biotechnol 31:839–843.

Rebecca MF, Vaishnavi A, Maruyama A, Deborah JA. 2013. Organ-specific gene expression: the bHLH protein Sage provides tissue specificity to *Drosophila* FoxA. Development 140:2160–2171.

Wang F, Xu H, Yuan L, Ma S, Wang Y, Duan X, Duan J, Xiang Z, Xia Q. 2013. An optimized sericin-1 expression system for mass-producing recombinant proteins in the middle silk glands of transgenic silkworms. Transgenic Res 22: 925–938.

Wang Y, Li Z, Xu J, Zeng B, Ling L, You L, Chen Y, Huang Y, Tan A. 2013. The CRISPR/Cas System mediates efficient genome engineering in *Bombyx mori*. Cell Res 23:1414–1416.

Wei W, Xin H, Roy B, Dai J, Miao Y, Gao G. 2014. Heritable genome editing with CRISPR/Cas9 in the silkworm *Bombyx mori*. PLOS ONE 9:e101210.

Xia Q, Guo Y, Zhang Z, Li D, Xuan Z, Li Z, Dai F, Li Y, Cheng D, Li R, Cheng T, Jiang T, Becquet C, Xu X, Liu C, Zha X, Fan W, Lin Y, Shen Y, Jiang L, Jensen J, Hellmann I, Tang S, Zhao P, Xu H, Yu C, Zhang G, Li J, Cao J, Liu S, He N, Zhou Y, Liu H, Zhao J, Ye C, Du Z, Pan G, Zhao A, Shao H, Zeng W, Wu P, Li C, Pan M, Li J, Yin X, Li D, Wang J, Zheng H, Wang W, Zhang X, Li S, Yang H, Lu C, Nielsen R, Zhou Z, Wang J, Xiang Z, Wang J. 2009. Complete resequencing of 40 genomes reveals domestication events and genes in silkworm (*Bombyx*). Science 326:433–436.

Xiao A, Cheng Z, Kong L, Zhu Z, Lin S, Gao G, Zhang B. 2014. CasOT: a genome-wide Cas9/sgRNA off-target searching tool. Bioinformatics 30:1180–1182.

Xu H, Yuan L, Wang F, Wang Y, Wang R, Song C, Xia Q, Zhao P. 2014. Overexpression of recombinant infectious bursal disease virus (IBDV) capsid protein VP2 in the middle silk gland of transgenic silkworm. Transgenic Res 23: 809–816.

Yu Z, Ren M, Wang Z, Zhang B, Rong Y, Jiao R, Gao G. 2013. Highly efficient genome modifications mediated by CRISPR/Cas9 in *Drosophila*. Genetics 195: 289–291.

Zhao A, Long D, Ma S, Xu L, Zhang M, Dai F, Xia Q, Lu C, Xiang Z. 2012. Efficient strategies for changing the diapause character of silkworm eggs and for the germline transformation of diapause silkworm strains. Insect Sci 19:172–182.

Zhao X, Liu C, Li Q, Hu W, Zhou M, Nie H, Zhang Y, Peng Z, Zhao P, Xia Q. 2014. Basic helix-loop-helix transcription factor Bmsage is involved in regulation of *fibroin H-chain* gene via interaction with SGF1 in *Bombyx mori*. PLOS ONE 9:e94091.